

Organic Synthesis | Hot Paper |

Stereodivergent Aminocatalytic Synthesis of *Z*- and *E*-Trisubstituted Double Bonds from AlkynalsLeyre Marzo,^[a] Javier Luis-Barrera,^[a] Rubén Mas-Ballesté,^[b] José Luis García Ruano,^[a] and José Alemán^{*[a]}

Abstract: A highly diastereoselective synthesis of trisubstituted *Z*- or *E*-enals, which are important intermediates in organic synthesis, as well as being present in natural products, is described using different alkynals and nucleophiles as starting materials. Diastereocontrol is mainly governed by the appropriate catalyst. Therefore, those reactions con-

trolled by steric effects, such as the Jørgensen–Hayashi's catalyst, give access to *E* isomers, and those catalysts that facilitate hydrogen bonding, such as tetrazol-pyrrolidine Ley's catalyst, allow the synthesis of *Z* isomers. A stereochemical model based on DFT calculations is proposed.

Introduction

The configuration of double bonds (*Z* or *E*) plays a central role in nature, for example, in fatty acids and also in the biological properties of different natural and pharmaceutical compounds.^[1] For example, (*Z*)-tamoxifen is an antiestrogen that inhibits the development and growth of mammary tumors in rats and is effective in treating estrogen-dependent metastatic breast cancer in humans.^[1b] By contrast, the diastereoisomer (*E*)-tamoxifen does not have any clinical uses because it lacks an antiestrogenic effect (A, Figure 1).^[1c] Other examples are the *E*- and *Z*-piperolides that exhibit different antimycotic activity against *Cladosporium cladosporoides*.^[1e] In addition, the *E*- and *Z*-propenones differ in their COX-2 inhibitory activity.^[1j] Furthermore, the stereochemical control of double-bond formation is critical for the synthesis of heterocycles, such as the lactame ring synthesis of the anticancer spirodinolinone derivatives **B**^[2] or the piran-2-one ring **C**^[3] with multiple biological properties (Figure 1). Therefore, the ability to control the configuration of a double bond is an extremely important task in the synthetic design of new drugs containing this structural moiety.

A detailed revision of the literature reveals that one of the best methods for the synthesis of olefins is the addition of nucleophiles to electron-deficient alkynes, which results in most cases, in mixtures of *Z/E* isomers.^[4] Different catalytic and non-catalytic additions have been performed, in some cases with

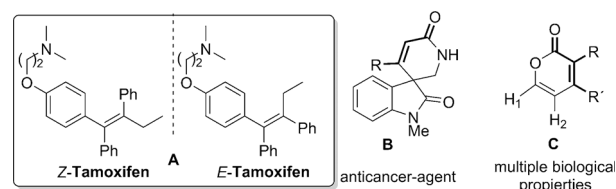


Figure 1. Structure and the importance in the *Z/E* control.

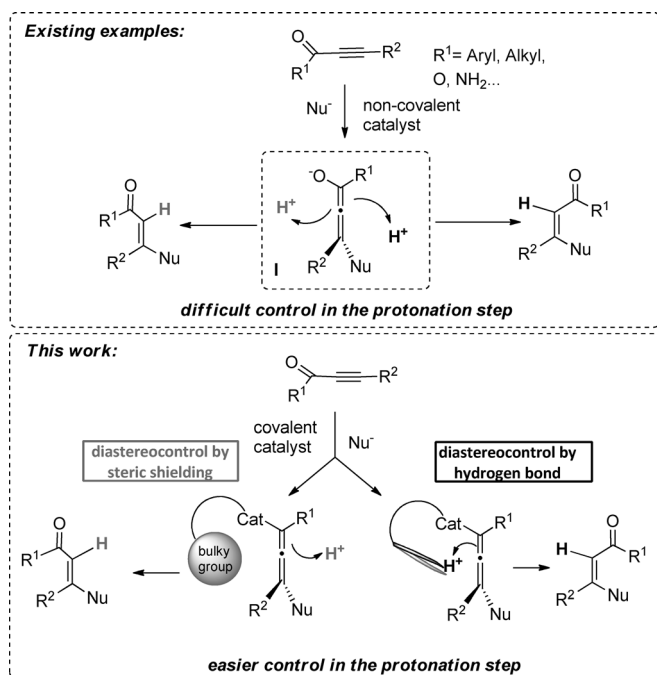
partial success for one of the two diastereoisomers. Most of the methods are designed for the addition to nonsubstituted terminal triple bonds ($R^2 = H$), yielding disubstituted double bonds (Scheme 1, top). Interestingly, when a terminally substituted triple bond is used ($R^2 \neq H$), the literature generally shows two types of additions with some degree of *Z/E* selectivity: 1) Michael reaction to alkynones that were reported to yield the *Z* adducts,^[5] and 2) alkynyl esters that generally presented *E* selectivity.^[6] Other additions cannot be governed with any selectivity.^[7] This poor control or lack of *Z/E* selectivity is related to the scarce stereochemical control in the facial recognition of the intermediary allenic enolate **I** (Scheme 1, top). Consequently, the design of *Z/E*-selective processes is still a challenge. Interestingly, stereodivergent systems for the synthesis of *Z* or *E* double bonds have not been described. Considering the intermediate **I** (Scheme 1, top), the selectivity problem is inherent in the protonation step, which is not controlled. Therefore, most authors have employed different catalytic systems to control, in an intermolecular manner, the protonation of the enolate intermediate **I**.

To increase the control in this process, it was envisioned that a catalyst directly attached to the intermediate **I** (i.e. covalently bonded) would increase control in the *Z/E* selectivity (Scheme 1, bottom) through a protonation step in an intermolecular (steric effect, Scheme 1, left-bottom) and intramolecular (hydrogen bond, Scheme 1, right-bottom) manner. Therefore, the use of an alkynal^[8] would allow the formation of the imini-

[a] Dr. L. Marzo, J. Luis-Barrera, Dr. J. L. G. Ruano, Dr. J. Alemán
Departamento de Química Orgánica, Universidad Autónoma de Madrid
Cantoblanco, 28049 Madrid (Spain)
E-mail: jose.aleman@uam.es
Homepage: www.uam.es/jose.aleman

[b] Dr. R. Mas-Ballesté
Departamento de Química Inorgánica, Universidad Autónoma de Madrid
Cantoblanco, 28049 Madrid (Spain)

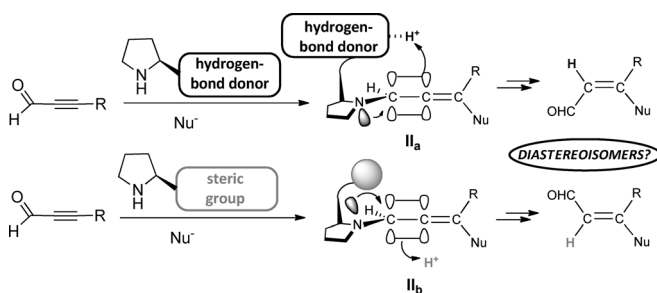
Supporting information for this article is available on the WWW under
<http://dx.doi.org/10.1002/chem.201603437>.



Scheme 1. Existing strategies for control in the *Z/E* selectivity and the proposed new strategy.

um ion that could be attacked by a nucleophile. The nucleophile chosen is a 1,3-dicarbonyl compound (commonly used in organocatalysis) that would enable the formation of the allenamine intermediate **II** (Scheme 2). Consequently, the control in the *Z* and *E* selectivity would be governed by an aminocatalyst (hydrogen-bond donor group, **II_a**, versus bulky group, **II_b**). Presumably, the use of a hydrogen-bond donor catalyst would facilitate the protonation at the same prochiral face at the hydrogen-bond group, whereas the use of a bulky group at the aminocatalyst would provoke a protonation at the opposite face to this group.

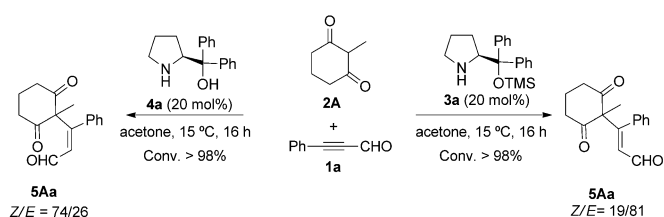
In this work, we report a new method for preparing *Z*- and *E*-trisubstituted olefins starting from alkynes with efficient diastereocontrol under organocatalytic conditions and propose a mechanistic stereochemical model based on DFT calculations.



Scheme 2. Proposal for the diastereo-divergency for alkynes through aminocatalysis.

Results and Discussion

To check *Z/E* selectivity in the nucleophilic addition to alkynes, the reaction between the 1,3 dicarbonyl compound **2A** and acetylenic derivative **1a**, in the presence of catalysts **3a** and **4a** was carried out. The use of **3a** (20 mol%) as a prototype of a steric-shielding catalyst in acetone preferentially led to the *E* isomer (*Z/E* = 19:81, Scheme 3, right-side). In contrast, when the reaction was carried out in the presence of a hydrogen-bond-type catalyst, such as the prolinol **4a**, the *Z* isomer was preferentially formed in the same solvent (*Z/E* = 74:26, Scheme 3, left-side), thus demonstrating our initial hypothesis. Interestingly, identical *Z/E* selectivity was obtained when using the enantiomers (*R* or *S*) of the catalysts **3a** and **4a**, or their racemic forms.



Scheme 3. First trials in the *Z/E* selectivity under aminocatalytic conditions.

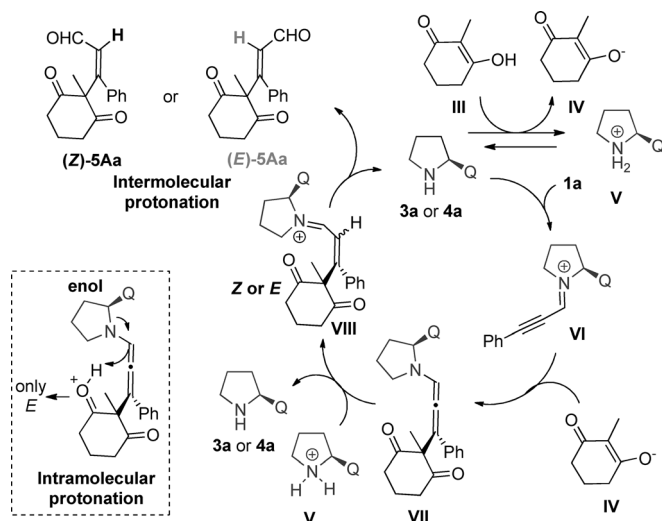
Mechanistic considerations: DFT calculations

To explain the observed *Z/E* regioselectivities, we addressed the theoretical investigation of the possible reaction pathways between the acetylene-containing iminium cationic species derived from catalysts **3a** or **4a**, and the corresponding nucleophile to generate the product **5Aa** (Scheme 3). Geometry optimizations were carried out using the M06 functional with 6-31G(d,p) basis set,^[9] including acetone solvent effects by means of a SMD continuum model, which is a standard methodology previously used for related aminocatalytic systems.^[9a] Electronic energies were refined by single-point calculations at M06/6-311++ + G(d,p) also including solvent effects. Energy values reported are given as increments of Gibbs free energies considering thermal corrections obtained at the M06/6-31G(p,d) level. The large dimensions of the calculated systems prevented the use of more sophisticated methods on both optimizations and thermal correction calculations (see the Supporting Information for additional details).

Initial and general considerations

A general picture of the plausible catalytic cycle is shown in Scheme 4. First, iminium ion formation **VI** would take place, which should be attacked by the enol **III** or enolate **IV** to form the allenamine intermediate **VII**. Such transient species (**VII**), although undetected, has also been proposed for related systems.^[8] Then, protonation of this allenamine **VII** would take place in an intramolecular (Scheme 4, bottom-left) or intermolecular manner (Scheme 4, top-left) to produce the correspond-

ing trisubstituted alkene **III**, precursor of **5Aa** (*E* or *Z*). Interestingly, the protonation was already proposed by Zimmerman in 1955 as the key step for the *Z/E* selectivity in the addition reaction of α,β -unsaturated carbonyl compounds via an allenol intermediate.^[10] In order to rationalize such a mechanistic proposal, each step of this reaction was separately considered: 1) acid–base equilibrium between the nucleophile and pyrrolidine catalyst, 2) iminium formation, 3) nucleophilic attack to the acetylenic species, and 4) protonation of the allenamine intermediate.



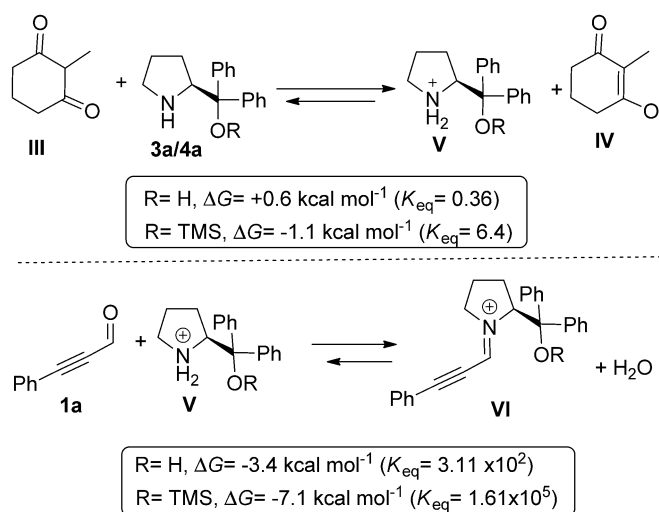
Scheme 4. General mechanistic scheme proposed in this work (Q=CPh₂OH or CPh₂OTMS).

Iminium formation and enol deprotonation

We initially assessed the thermodynamic feasibility of the two prior processes: acid–base equilibrium between the nucleophile and pyrrolidine catalyst and iminium formation. The pyrrolidine catalyst can act as a base (from **3a** or **4a** to **V**, Scheme 5, top) and the deprotonation of the nucleophile is feasible with both catalysts **3a** and **4a** ($\Delta G = +0.6 \text{ kcal mol}^{-1}$, $K_{\text{eq}} = 0.36$ and $\Delta G = -1.1 \text{ kcal mol}^{-1}$, $K_{\text{eq}} = 6.4$, respectively), which is in agreement with the lower nucleophilicity of catalyst **3a**. The formation of the iminium ion **VI** from **V** and **1a** is clearly favored for catalysts **3a** and **4b** (Scheme 5, bottom). Remarkably, formation of each iminium **VI** implies the consumption of a proton to form a water molecule, which would be the pyrrolidinium salt **V**, previously formed by deprotonation of **III** by **3a** or **4a**. Once the iminium ion **VI** was formed, a nucleophilic attack from the enol **III** or enolate **IV** would take place.

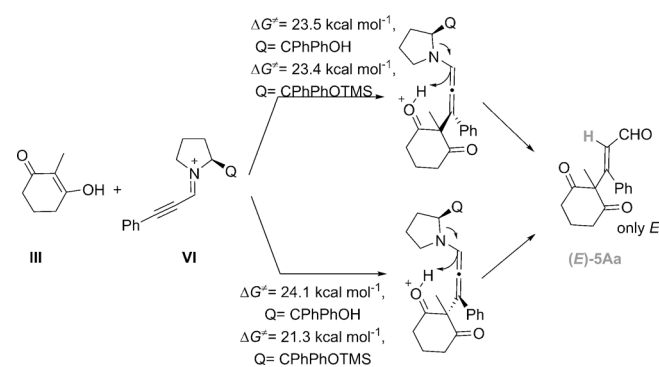
Nucleophilic attack

A first possible pathway is the enol formation (**III**) and a further attack on the acetylenic iminium intermediate **VI**, followed by proton transfer to produce the corresponding trisubstituted alkene **5Aa** (Scheme 6). Such a pathway is not relevant be-



Scheme 5. Deprotonation of the enol by the catalyst and formation of the iminium ion.

cause the attack of the enol **III** on the iminium ion **VI** proceeds through high energetic barriers (between 21.3 and 24.1 kcal mol⁻¹, see Scheme 6 and the Supporting Information). Furthermore, the intramolecular protonation should proceed from the enol fragment to the acetylene moiety and this mechanism can only account for the *E* product and cannot explain the formation of *Z* products.



Scheme 6. Enol attack to the iminium ion and intramolecular protonation to give (*E*)-**5Aa** (Q=CPh₂OH or CPh₂OTMS).

A more plausible addition is related to the attack of the enolate **IV** to the iminium ion **VI**, leading to thermodynamically favorable allenamine intermediates with low kinetic barriers ($\Delta G^\ddagger =$ from 4.2 to 6.1 kcal mol⁻¹, see Figures 4 and 6). The nucleophilic attack of the enolate **IV** on the iminium ion **VI** can proceed in two different orientations and leads to the allenamines **VII** and **VII'** under the catalysis of **3a** or **4a** (Figures 2 and 3, respectively). For each allenamine another plausible rotation in the C–N bond can take place, giving two additional structures **VII-rot** and **VII'-rot**.

Protonation of these species gives access to the final double bonds. The protonation source should be the pyrrolidinium ion

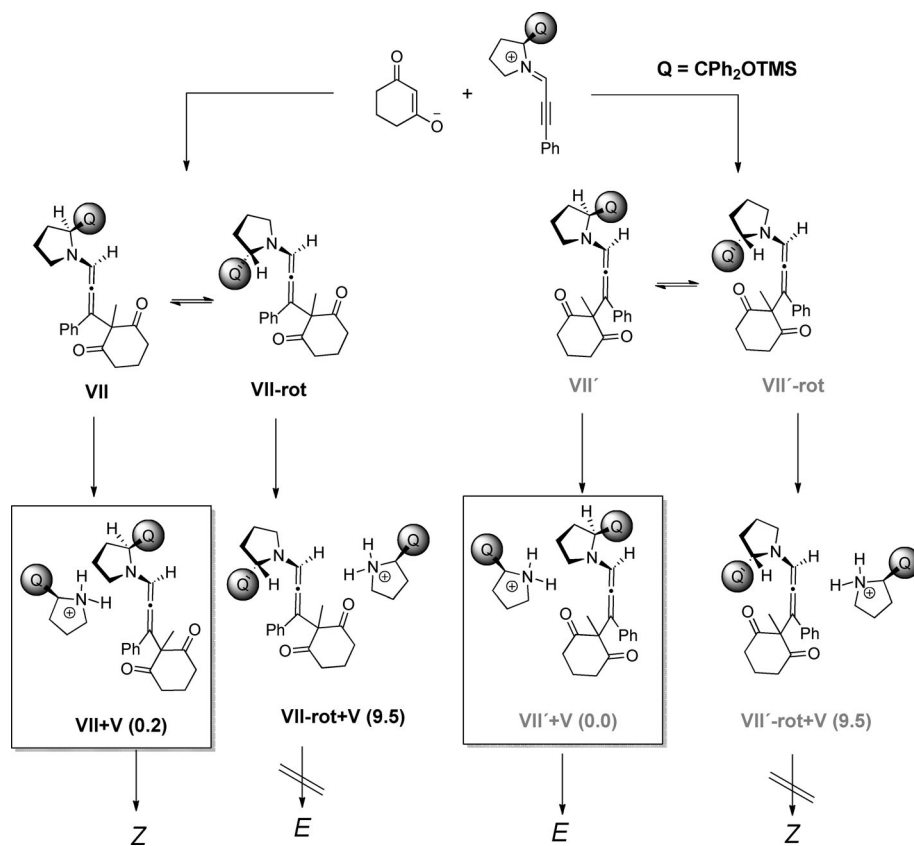


Figure 2. Analysis in the approach of the pyrrolidinium ion to the allenamine intermediate (Q=CPhPhOTMS). Stabilities in kcal mol⁻¹ are shown in brackets.

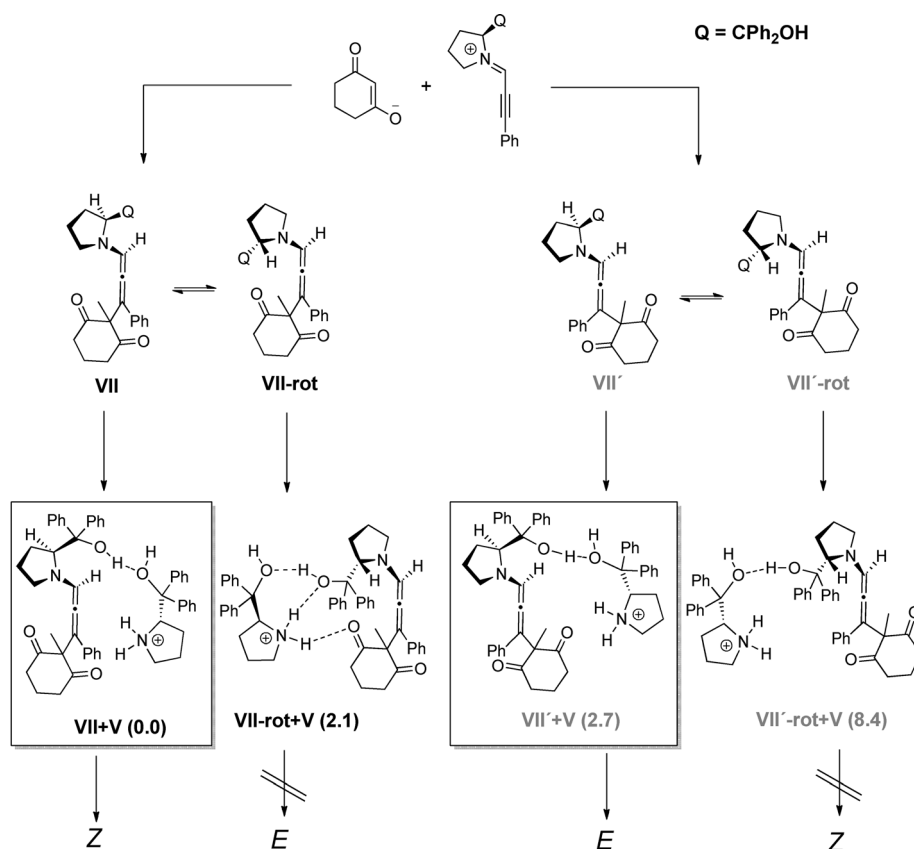


Figure 3. Analysis in the approach of the pyrrolidinium ion to the allenamine intermediate (Q=CPh₂OH). Stabilities in kcal mol⁻¹ are shown in brackets.

(V), which is the more acid proton in the media (Figure 2, top left, and Figure 3). A detailed analysis in the approach of the pyrroldinium ion to the allenamines reveals that only two of the four dispositions can give access to the final double bonds, since the free energies of these intermediates are very high or access to the proton source is not adequate (for values in brackets, see the Supporting Information for more details). Therefore, the energetic profiles of the plausible pathways (VII and VII' allenamine intermediates) for both catalysts 3a and 4a were analyzed.

Energetic profile for catalyst 4a—kinetic control

The energetic profiles shown in this and subsequent sections start from iminium and enolate ion pairs. Two main steps are analyzed from both thermodynamic and kinetic perspectives: First the nucleophilic attack of enolate to acetylenic iminium species to form allenamine intermediate and, second, the protonation of these allenamines by pyrroldinium cation V according the geometries presented in Figures 2 and 3.

For catalyst 4a, the nucleophilic attack of the enolate IV on the iminium ion VI can proceed in two different orientations (Figure 4); from TS-VI to form VII or from TS-VI' to generate VII' (nucleophilic addition step). Such processes (TSVI and TSVI' Figure 4) are thermodynamically allowed ($\Delta G_{\text{react}} = -14.9$ and $-14.8 \text{ kcal mol}^{-1}$) and both products are produced through a very similar kinetic barrier ($4.3 \text{ kcal mol}^{-1}$ for VII and $4.2 \text{ kcal mol}^{-1}$ for VII', Figure 4).

In this first step there is not a significant differentiation of the two pathways from either kinetic or thermodynamic points of view. Therefore, the key to the diastereo-differentiation should be related to the protonation step of these allenamine intermediates. An analysis of the protonation step according to the catalyst 4a is described below. Firstly, a hydrogen bonding between the two pyrrolidine moieties was found, one as the proton source and the other in the allenamine fragment (TSVII and TSVII', Figure 5). From the allenamine intermediates VII or VII', alkene final products are generated by protonation using pyrroldinium cation V as the proton source (previously formed from 4a by deprotonation, see Scheme 5). As a consequence of $\Delta G^{\ddagger 4}$ being larger than $\Delta G^{\ddagger 3}$, the formation of VIII is favored under kinetic control, as the protonation orientation is the determining factor in the Z/E selectivity (Figure 4, top). As can be deduced from the reaction profile (Figure 4), kinetic control results from the difference of the activation energies ($\Delta G^{\ddagger 4} - \Delta G^{\ddagger 3} = 1.9 \text{ kcal mol}^{-1}$, the pro-Z transition state (TSVII) and the pro-E transition state (TSVII'), which is in accordance with the moderate diastereoselectivity that was obtained in the case of the Z product (74:26 Z/E, Scheme 3). This difference of energy is even larger when the entropic cost (VII + V and VII' + V) is considered.

Grey and black traces in the profile shown at Figure 4 are related to the two steps of two catalytic cycles that could work and result on formation of Z and E products, respectively. The corresponding turnover frequency of these two alternative catalytic cycles (grey or black traces) depends on the successive kinetic barriers, as the energy of these barriers is the factor

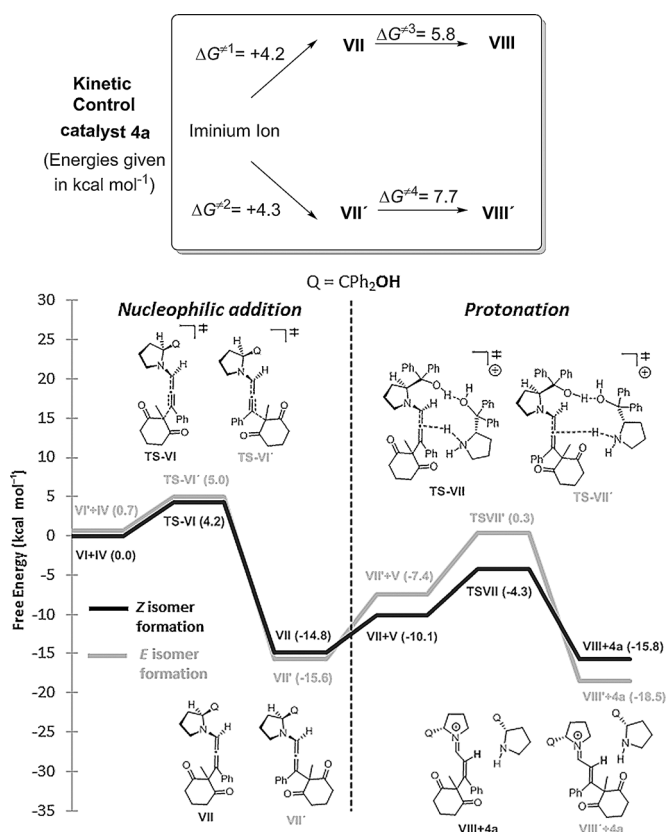


Figure 4. Energetic profile of the reaction pathway followed using catalyst 4a (Q = CPh₂OH). The zero value is established at the VI + IV ion pair.

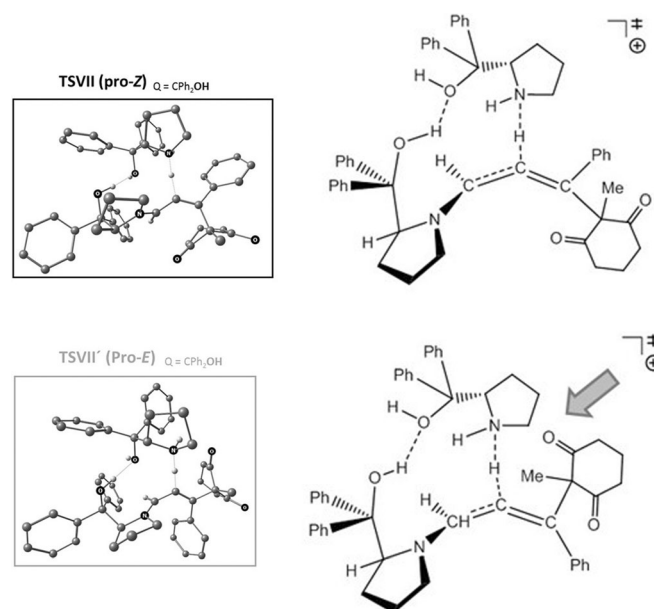


Figure 5. Transition states for the protonation step of the allenamine intermediate by protonated catalyst 4a. The grey arrow points out the steric hindrance region.

that determines the rate at which the catalytic cycle is completed. In this case, the two calculated barriers for the pro-Z pathway are $4.2 \text{ kcal mol}^{-1}$ for the nucleophilic attack and

5.8 kcal mol⁻¹ for the protonation step (black trace). For the pro-*E* pathway, grey trace, a higher barrier has been found for the protonation process (7.7 kcal mol⁻¹; see Figure 4, top), whereas a very similar value has been computed for the barrier of nucleophilic attack (4.3 kcal mol⁻¹). Therefore, it is clear that the rate-determining step is the protonation, in which a significant difference is found between *Z* (black trace) and *E* cycles (grey trace). In fact, the *Z* cycle is kinetically preferred over the *E* cycle, and, therefore, a higher turnover frequency is expected for the *Z* cycle, which should have, as a consequence, a higher accumulation of *Z* product. Geometrical analysis of both pro-*E* and pro-*Z* transition states (shown in Figure 5) suggests that steric hindrance between the nucleophilic fragment and the pyrrolidinium proton donor make the **TSVII'** transition state (pro-*E*) less favorable than **TSVII** transition state (pro-*Z*).

Energetic profile for catalyst 3a—thermodynamic control

Although the nucleophilic attack step does not show significantly distinct thermodynamic or kinetic features for the *Z* or *E* cycles, a different scenario was found in the protonation step for the reaction catalyzed by **3a** (Figure 6). Due to the steric crowding, the only orientation of the -CPh₂OTMS group of the allenamine intermediate **VII** and **VII'** should be at the opposite site of this bulky group in the protonation reagent **V** (see **TSVII** and **TSVII'**, Figure 6). Due to the relative orientation of the -CPh₂OTMS groups, steric hindrance between the nucleo-

philic fragment and the pyrrolidinium proton donor in the pro-*E* transition state (**TSVII'**) is, in this case, comparable to the steric hindrance between the -CPh₂OTMS group of the allenamine and the nucleophilic fragment in the pro-*Z* transition state (**TSVII**) (see Figure 7). Therefore, in this case, there is not a kinetic preference (the energy barrier for **TSVII'** is only 0.4 kcal mol⁻¹ more stable than the barrier for **TSVII**, see Figure 3). Consequently, the preference for the *E* product should be understood in the context of thermodynamic control. Indeed, the *E* isomer is, in this case, about 6.2 kcal mol⁻¹ more stable than its *Z* counterpart (vide infra).

This thermodynamic control requires reversibility in the different steps of the catalytic cycle. Once intermediates **VII** or **VII'** are generated, the reversibility at this step would require overcoming barriers of 18.5 and 19.7 kcal mol⁻¹ ($\Delta G^{\ddagger 1}$ and $\Delta G^{\ddagger 2}$; from **VII** or **VII'** to **VI** or **VI'**, respectively, to the iminium ion, Figure 4, top). Considering these values, such reversibility is plausible especially at higher temperatures and longer reaction times. In addition, overall barriers from **VII** (**TSVII**) and **VII'** (**TSVII'**) should include the entropic costs of forming the **VII** + **V** and **VII'** + **V** pairs which are not very distinct from $\Delta G^{\ddagger 1}$ and $\Delta G^{\ddagger 2}$. Furthermore, the scarce availability of the pyrrolidinium ion is limited by the prior equilibria (acid-base equilibrium between nucleophile and pyrrolidine catalyst and iminium formation) making the path from **VII** or **VII'** to **TSVII** or **TSVII'**, even

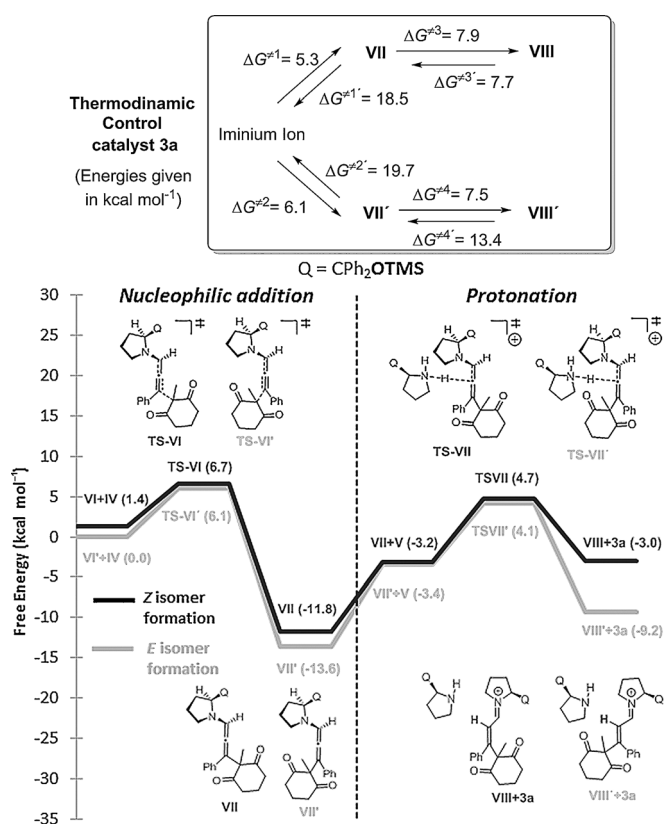


Figure 6. Energetic profile of the reaction pathway followed using catalyst **3a** (Q = CPh₂OTMS). The zero value is established at the **VI**+**IV** ion pair.

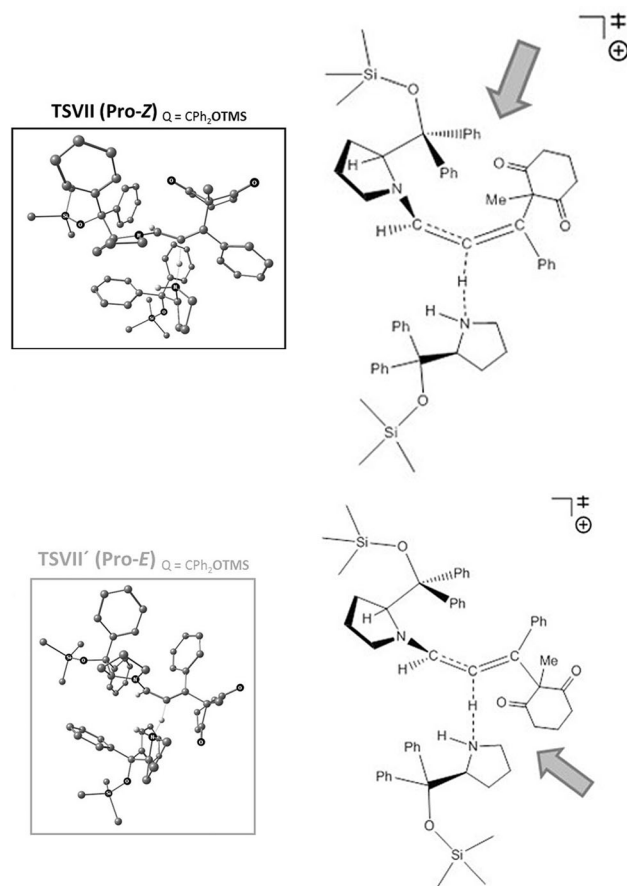


Figure 7. Transition states for protonation step of the allenamine intermediate by protonated catalyst **3a**. The grey arrows point out steric hindrance regions.

slower, and then reversibility from **VII** to **VI** or from **VII'** to **VI'** more probable. From **VIII** to **VII**, reversibility is quite plausible considering the almost equally low values of $\Delta G^{\ddagger 3}$ (7.9 kcal mol⁻¹) and $\Delta G^{\ddagger 3'}$ (7.7 kcal mol⁻¹). In contrast, reversibility from **VIII'** to **VII'** should be less favorable because $\Delta G^{\ddagger 4}$ (7.5 kcal mol⁻¹) is considerably lower than $\Delta G^{\ddagger 4'}$ (13.4 kcal mol⁻¹). Therefore, the irreversible pathway initiated by dissociation of the **VIII**+**3a** pair and finished by imine hydrolysis is more probable. Thus, accumulation of the thermodynamically favored product is expected.

The general thermodynamic preference for the *E* product can be understood when considering how the steric interactions in **VIII** and **VIII'** can affect the conjugation in the fragment N=C(H)-C(H)=C(Ph)(Nuc) (Figure 8). When catalyst **4a** is used the dihedral angle H-C-C-H is 179° for the *E* product (**VIII'**) and 174° for the *Z* product (**VIII**). This loss of planarity (ideally 180°), and therefore lack of conjugation, is related to a destabilization of 4.2 kcal mol⁻¹ for the *Z* product (**VIII**). This effect is enhanced by using the more sterically hindered catalyst **3a**. In this case, the dihedral angle H-C-C-H is 172° for the *E* product (**VIII'**) and 159° for the *Z* product (**VIII**). Therefore, the *E* product (**VIII'**) is 6.9 kcal mol⁻¹ more stable than its *Z* counterpart.

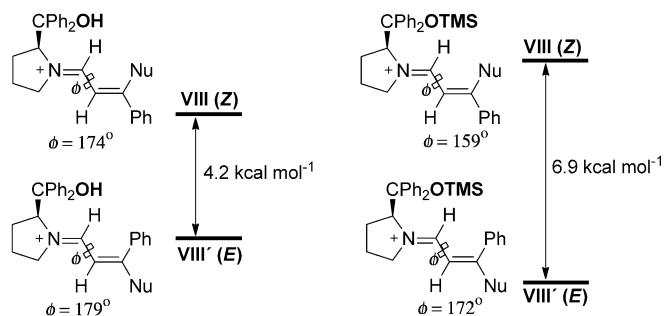
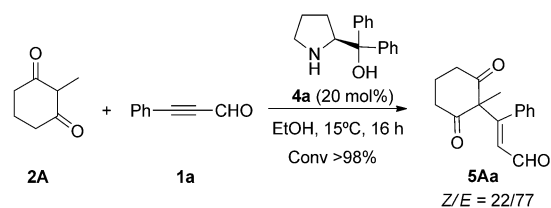


Figure 8. A comparison of the thermodynamic stability of isomers *E* and *Z* with **4a** catalyst (left) and **3a** catalyst (right).

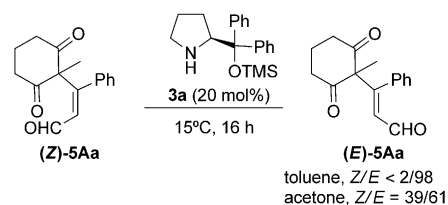
Experimental proof supporting the mechanistic proposal

According to the calculations mentioned above, the hydrogen bond under the catalysis of **4a** is critical to obtain the *Z*-enal **5Aa**. To test this hypothesis, the reaction was carried out in ethanol, which is able to break these intermolecular hydrogen bonds (see Figure 4). The opposite configuration (*E*) was found in ethanol due to a steric control taking place (Scheme 7).

To gain a better understanding of the catalyst **3a**, we dissolved a pure sample of the *Z* product (obtained by kinetic control) in toluene or acetone in the presence of catalyst **3a** in order to perform the reaction under thermodynamic control conditions. As expected, the reaction reached thermodynamic equilibrium and the isomerization of the *E* product took place, which was partial in acetone but complete in toluene as the solvent (Scheme 8). This experimental evidence confirms that catalyst **3a** promotes thermodynamic control through a reversible pathway.



Scheme 7. Effect of ethanol on the diastereoselectivity.



Scheme 8. Isomerization of (*Z*)-**5Aa** in the presence of **3a**.

According to our mechanistic proposal, kinetic control using catalyst **4a** should be enhanced by lowering the temperature, whereas thermodynamic control using catalyst **3a** should be enhanced by raising the temperature (Figure 9). Indeed, when the reaction using catalyst **4a** was carried out at 0°C (kinetic control, Figure 9, left) 86% of the *Z* isomer was obtained, whereas this was decreased to 60% at 40°C. In the case of catalyst **3a** (thermodynamic control, Figure 9, right), the reaction was found to decrease the amount of *E* product when the reaction was carried out at 0°C (68%) in comparison to the selectivity found at 40°C (98% of the *E* isomer). Therefore, the influence of the temperature in the kinetic and thermodynamic control in combination with the structure of the catalysts (**3a** and **4a**) are the principal factors that determines the observed *Z/E* ratio.

Screening conditions and scope

With these computational studies and the preliminary results obtained, the reaction conditions for the diastereoselective synthesis of the *E* or *Z* isomers were optimized with a more reactive nucleophile **2B** (Table 1). In the absence of the catalyst, the reaction did not take place after 48 h in toluene at 15°C (entry 1, Table 1). For the selective preparation of the *E* isomer, different catalysts bearing bulky substituents were studied in toluene at 15°C (entries 2–6). The best results in toluene were obtained with the bulkier ones (**3b** and **3f**, entries 2 and 6). The influence of the solvent was then studied using **3b** (entries 7–10). EtOH provided the best diastereoselectivity with **3b** and **3f** (*Z/E*=3:97, entries 8 and 14). At this point we checked whether a decrease in the temperature (0 or –20°C) would reduce the diastereoselectivity (which would be expected for a major product resulting from thermodynamic control) (entries 11–12), and whether a dilution in the reaction conditions had any influence (entry 13). Finally, a decrease in the catalyst loading to 10 or 5 mol% resulted in a lower reactivity and diastereoselectivity (entries 15 and 16). Interestingly, the results

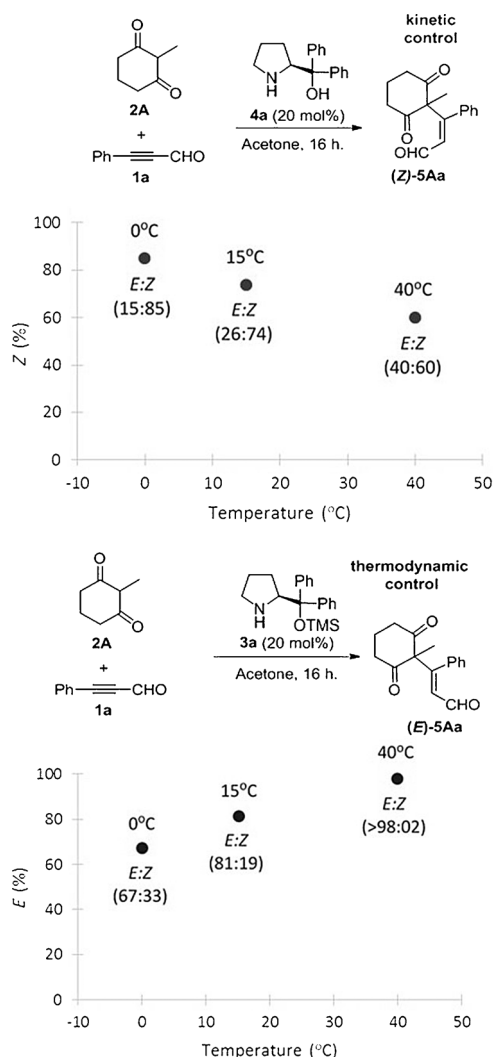


Figure 9. Reactions under **3a** and **4a** catalysts under different temperatures.

obtained in the reaction of **1a** with **2A** were identical to those using (*R*)-**3b**, (*S*)-**3b**, or (\pm)-**3b** as the catalyst. Therefore, the cheaper catalyst (*S*)-**3b** was employed in further experiments.^[11] From the results in Table 1, we chose the conditions of entries 8 and 14 as optimal for achieving the *E* isomers of the trisubstituted olefins with the best diastereoselectivity. Under these conditions, the reactions of **1a** with nucleophiles (**2A–G**) were studied. The results are depicted in Table 2.

The nucleophiles **2B** and **2C** yielded (*E*)-**5Ba** and (*E*)-**5Ca**, respectively, as the unique diastereoisomers (Table 2), but the use of toluene as the solvent was required in the second case. Similarly, diastereoselectivity was complete in reactions with **2E** and **2A**, whereas **5Da** and **5Fa** were obtained in toluene at a 15:85 and 25:75 mixture, respectively (Table 2). This result could not be improved by using **3f** as the catalyst. Finally, the Meldrum acid derivative **2G** yielded the trisubstituted olefin (*E*)-**5Ga** (72%) as a unique diastereoisomer.

At this point, the scope of the reaction with different alkyls was studied (Table 3). We found that under the conditions of entry 8 in Table 1, very good results were achieved from β -aryl alkynals, which only yielded the *E* isomer when electron-

Table 1. Optimization in the reaction of nucleophile **2B** and aldehyde **1a** in the presence of catalyst **3**.^[a]

Entry	Cat [mol%]	Solvent	t [h]	T [°C]	Conv. [%] ^[b]	Z/E [%] ^[c]
1	–	Tol.	48	15	–	–
2	3b (20%)	Tol.	16	15	> 98	10:90
3	3c (20%)	Tol.	16	15	> 98	12:88
4	3d (20%)	Tol.	16	15	> 98	44:56
5	3e (20%)	Tol.	16	15	> 98	46:54
6	3f (20%)	Tol.	17	15	> 98	6:94
7	3b (20%)	CH ₂ CN	24	20	> 98	7:93
8	3b (20%)	EtOH	24	20	> 98	3:97
9	3b (20%)	THF	24	20	> 98	8:92
10	3b (20%)	CH ₂ Cl ₂	24	20	> 98	12:88
11	3b (20%)	EtOH	20	0	> 98	8:92
12	3b (20%)	EtOH	20	-20	90	20:80
13	3b (20%)	EtOH ^[d]	18	15	> 98	3:97
14	3f (20%)	EtOH	16	20	> 98	3:97
15	3b (10%)	EtOH	20	15	94	6:94
16	3b (5%)	EtOH	20	15	60	7:93

[a] All reactions were performed using 0.1 mmol of **2B** and 0.2 mmol of **1a**, in 0.2 mL of solvent. [b] Conversion was determined by ¹H NMR. [c] Z/E ratio was determined by ¹H NMR. [d] Diluted up to 0.1 M. Tol. = toluene

Table 2. Scope of the nucleophiles under optimal conditions for the diastereoselective preparation of the *E* isomers starting from **1a**.^[a,b]

(E)-5Aa (83%) ^[c] Z/E = >2/98	(E)-5Ba (96%) Z/E = 3/97	(E)-5Ca (61%) ^[c] Z/E = >2/98	(E)-5Da (70%) ^[c] Z/E = 15/85
(E)-5Ea (59%) Z/E = >2/98	(E)-5Fa (73%) ^[c] Z/E = 25/75	(E)-5Ga (72%) Z/E = >2/98	

[a] All the reactions were performed using 0.1 mmol of **2** and 0.2 mmol of **1** in 0.2 mL EtOH at 15 °C. [b] Z/E ratio was determined by ¹H NMR. [c] This reaction was carried out in 0.2 mL of toluene.

donating substituents were present in the aryl group (**5Bb** and **5Bc**) and highly selective *E/Z* ratios when electron-withdrawing and *ortho*-substituents were used (**5Bd** and **5Be**). In the alkyl

groups, slightly worse results were found. Using **1 g** (R = *n*-pentyl) and **1 h** (R = cyclohexyl) produced 6:94 (61% yield) and 14:86 (73% yield) using **3 f** as the catalyst. However, **1 i** did not react (probably due to the strong steric restrictions of the tertiary alkyl groups), whereas a lower stereoselectivity was obtained from the β -cyclohexenyl enal **1 f**, resulting in a 31:69 mixture of isomers under the catalysis of **3 f** (Table 3).

Table 3. Scope of alkynals under optimal conditions for the diastereoselective preparation of the *E* isomers starting from **2 B**.^[a,b]

[c] Z/E = 12/88 (6/94) ^[d]				

[a] All reactions were performed with 0.1 mmol of **2**, 0.2 mmol of **1**, and 20 mol% of catalyst **3 b** in 0.2 mL of EtOH at 15 °C. [b] Z/E ratio was determined by ¹H NMR. [c] The Wittig reaction product was isolated. [d] Obtained using **3 f** as the catalyst.

For the optimization of the conditions providing *Z* isomers as the major components of the reaction mixtures, we also chose the reaction between **1 a** and **2 B** in toluene at 15 °C (Table 4). Firstly, we studied the influence of different catalysts bearing acid protons (entries 1–5, Table 4). The reaction did not take place in the presence of **4 b** and **4 c** (entries 2 and 3, Table 4), whereas **4 a** (entry 1), **4 d** (entry 4), and **4 e** (entry 5) were found to be efficient catalysts, yielding mixtures of geometric isomers (with *Z* being predominant) with moderate selectivity. As the reactivity was higher with **4 d** (the only one that provided full conversion after 16 h) it was initially chosen for the rest of the optimization experiments. A decrease in the reaction temperature to 0 °C resulted in a higher diastereoselectivity (as expected for a major product coming from kinetic control) but with a lower conversion (entry 6, Table 4). Different solvents were studied under the catalysis of **4 d** at 15 °C (entries 7–11). The reaction did not take place in EtOH (entry 7), whereas the conversion was complete in aprotic solvents (entries 8–11), with THF giving the best Z/E ratio (90:10, entry 11). As **4 a** and **4 e** had shown higher stereoselectivity control than **4 d** in toluene, their reactions were also studied in THF, but the results were unsuccessful (compare entries 12 and 13 with 11). Finally, a dilution to 0.1 M in THF at 15 °C improved the results at entry 11, providing a full conversion and a Z/E ratio of 92:8 (entry 14).^[12] These conditions were chosen as the most appropriate for the diastereoselective synthesis of the *Z*-trisubstituted olefins. The scope of the reaction of **1 a** with different nu-

cleophiles (**2 A–F**) to form the (*Z*)-**5** isomers, under the conditions of entry 14 of Table 4, was investigated (Table 5).

β -Ketoesters **2 B–D** were stereoselectively transformed in high yields into isomer mixtures, in which *Z* was clearly predominant (diastereomeric ratios better than 91:9). The azlactone **2 E** evolved into a modest 28:72 ratio of **5 EA** (83% yield)^[13] and β -diketones **2 A** and **2 F** were produced in yields of 77:23 (61% yield) and 90:10 (96% yield) mixtures of *Z/E* isomers, respectively (Table 5).

Table 4. Optimization of the reaction of **1 a** with **2 B** to give (*Z*)-**5**.^[a]

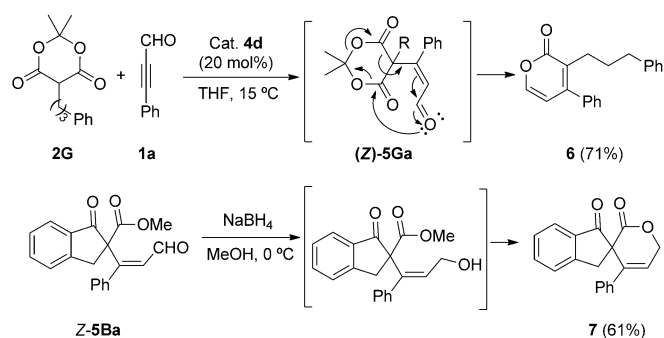
Entry	Cat [mol %]	Solvent	t [h]	T [°C]	Conv. [%] ^[b]	Z/E [%] ^[c]
1	4 a (20%)	Tol.	16	15	63	76:24
2	4 b (20%)	Tol.	16	15	no reaction	–
3	4 c (20%)	Tol.	16	15	no reaction	–
4	4 d (20%)	Tol.	16	15	> 98	63:37
5	4 e (20%)	Tol.	16	15	59	83:27
6	4 d (20%)	Tol.	16	0	53	77:23
7	4 d (20%)	EtOH	20	15	no reaction	– ^[e]
8	4 d (20%)	DCE	20	15	> 98	76:24
9	4 d (20%)	CH ₂ Cl ₂	20	15	> 98	77:23
10	4 d (20%)	CHCl ₃	20	15	> 98	80:20
11	4 d (20%)	THF	20	15	> 98	90:10
12	4 a (20%)	THF	20	18	no reaction	–
13	4 e (20%)	THF	20	18	> 98	86:14
14	4 d (20%)	THF ^[d]	18	15	> 98	92:8

[a] All reactions were performed on a 0.1 mmol scale of **2 B** in 0.2 mL solvent. [b] Conversion was determined by ¹H NMR. [c] Z/E ratio was determined by ¹H NMR. [d] Diluted to 0.1 M. [e] Catalyst was not completely soluble.

Table 5. Scope of the nucleophiles under optimal conditions for the diastereoselective preparation of the *Z* isomers starting from **1 a**.^[a,b]

[a] All reactions were performed with 0.1 mmol of **2** and 0.2 mmol of **1** in 1 mL THF at 15 °C. [b] Z/E ratio was determined by ¹H NMR. [c] Isolated as Wittig's reaction product.

The results obtained in the reaction of **1a** with the Meldrum's derivative **2G** (Scheme 9, top) under conditions favoring the formation of the *Z* isomers merit special comment. Instead of the expected compound (*Z*)-**5Ga**, pyrone **6**^[14] was exclusively obtained in a high yield, as a consequence of the rearrangement exerted by the aldehyde. This is an important result taking into account that pyran-2-ones, such as **C** (Figure 1) are important biological targets. The rearrangement indicated in Scheme 9 could not take place from the olefin of the *E* configuration because the spatial arrangement of the formyl group would not be appropriated. Therefore, compound (*E*)-**5Ga** could easily be isolated under the conditions in Table 2. Another interesting example that highlights the importance of the configuration of the double bond is outlined at the bottom of Scheme 9. Thus, only the *Z* configuration of **5Ba** is able to have the appropriated configuration to cyclize and give the spiro-compound **7**, which is presented in several natural products.^[15]



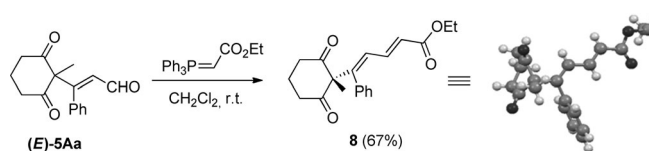
Scheme 9. Reaction of **2G** with **1a** under catalysis of **4d** and reduction of (*Z*)-**5Ba**.

The scope of the reaction of **2B** with different alkynals (**1a–i**) to form the *Z*-**5** isomers, under the conditions in entry 14 of Table 4, was also investigated (Table 6). β -Aryl alkynals usually provided high yields and very good selectivity, regardless the electronic character and the position of the aryl substituents. The reaction with **1i** did not work (as has been observed in other publications^[8]), whereas **1g** (*R* = *n*-pentyl) and **1h** (*R* = cyclohexyl) resulted in 57:43 (56% yield) and 80:20 (37% yield) mixtures, with the *Z* isomer being predominant, thereby suggesting some positive influence of the size of the substituent on the stereoselectivity, which contrasts with the tendency shown in Table 3. Finally, the β -cyclohexenyl alkynal **1f** produced (*Z*)-**5Bf** as the only isomer with an excellent yield (89%), which also contrasts with the scarce stereoselective evolution of this alkynal under the conditions in Table 3.

The configurational assignment of the double bonds present in compound **5** was unequivocally established by NMR and X-ray diffraction studies. The configuration (*E*) of the double bond was unequivocally assigned by X-ray diffraction studies of compound **8**,^[16] synthesized from (*E*)-**5Aa** by Wittig reaction with the appropriated phosphorous ylide (Scheme 10).^[17]

Table 6. Scope of alkynals under optimal conditions for the diastereoselective preparation of the *E* isomers starting from **2B**.^[a,b]

 (<i>Z</i>)- 5Ba (95%) Z/E = 91/9	 (<i>Z</i>)- 5Bb (97%) Z/E = >98/2	 (<i>Z</i>)- 5Bc (99%) Z/E = 91/9	 (<i>Z</i>)- 5Bd (74%) Z/E = 87/13	 (<i>Z</i>)- 5Be (62%) Z/E = >98/2
 (<i>Z</i>)- 5Bf (89%) Z/E = >98/2	 (<i>Z</i>)- 5Bg (56%) ^[c] Z/E = 57/43	 (<i>Z</i>)- 5Bh (37%) ^[c] Z/E = 80/20	 (<i>Z</i>)- 5Bi n.r.	
<p>[a] All reactions were performed with 0.1 mmol 2 and 0.2 mmol 1 in 1 mL THF at 15 °C. [b] Z/E ratio was determined by ¹H NMR. [c] The corresponding Wittig reaction product was isolated.</p>				



Scheme 10. Derivatization of (*E*)-**5Aa** and X-ray structure of compound **8**.

Conclusion

In conclusion, we have presented here a highly diastereoselective synthesis of trisubstituted *Z* or *E* enals by using different alkynals and nucleophiles as starting materials. The diastereocontrol is mainly governed by the catalyst used. Thus, reactions controlled by steric effects, like Jørgensen–Hayashi's catalyst, give access to *E* isomers through thermodynamic control, whereas catalysts such as tetrazol-pyrrolidine Ley's catalyst allow the synthesis of *Z* isomers, preferably obtained by means of kinetic control. The combination of experimental and theoretical work points towards the protonation of allenamine intermediates as the key step in the case of the kinetic products *Z*, whereas in the case of the *E* products the thermodynamic control shifts the equilibrium to the more stable isomer. Although protonation steps are generally considered as low barrier nonselective processes, in the kinetic control, the formation of the putative pyrrolidinium species as protonation agents allows the generation of distinct kinetic barriers that, in part, depend on the different steric interactions generated in the protonation process. Otherwise, diastereoselectivity arises from thermodynamic control due to distinct steric repulsions on pro-*E* and pro-*Z* iminium intermediates. The reaction allows the synthesis of a large variety of trisubstituted-enals from different alkynals and 1,3-dicarbonyl derivatives, achieving in all the cases from moderate to excellent diastereoselectivities. In addition, by choosing the appropriate catalyst, the synthesis of

the *Z* or *E* enals can be achieved, making this methodology attractive for the synthesis of trisubstituted double bonds.

Experimental Section

Experimental procedures, complete screening tables, NMR spectra of all new compounds, SFC chromatograms, and computational data are reported in the Supporting Information.

Acknowledgements

Financial support from the Spanish Government (CTQ2015-64561-R, CTQ-2012-37420-C02-02 and CTQ-2012-35957) is gratefully acknowledged. J.A. thanks the MICINN for the 'Ramon y Cajal' contract. We gratefully acknowledge computational time provided by the CCC (UAM). We thank P. SanLazaro for the initial experiments in this work.

Keywords: alkynals · aminocatalysis · double bonds · enals · protonation

- [1] For compounds with different biological properties depending on the double bond stereochemistry, see: a) N. Redwane, H. B. Lazrek, J. L. Barascut, J. L. Imbach, J. Balzarini, M. Witvrouw, E. De Clerq, *Nucleosides Nucleotides Nucleic Acids* **2001**, *20*, 1439; b) D. W. Robertson, J. A. Katzenellenbogen, *J. Org. Chem.* **1982**, *47*, 2387; c) C. Arellano, B. Allal, A. Goubaa, H. Roché, E. Chatelut, *J. Pharm. Biomed. Anal.* **2014**, *100*, 254; d) S. Nanda, A. I. Scott, *Tetrahedron: Asymmetry* **2004**, *15*, 963; e) J. H. G. Lago, T. M. Tanizaki, M. C. M. Young, E. F. Guimarães, M. J. Kato, *J. Braz. Chem. Soc.* **2005**, *16*, 153; f) Y. Tang, R. Muthyala, R. Vince, *Bioorg. Med. Chem.* **2006**, *14*, 5866; g) V. Devreux, J. Wiesner, H. Jomaa, J. V. Eycken, S. V. Calenbergh, *Bioorg. Med. Chem.* **2007**, *17*, 4920; h) S. Zhou, M. N. Prichard, J. Zemlicka, *Tetrahedron* **2007**, *63*, 9406; i) B. Modzelewska-Banachiewicz, B. Michalec, T. Kaminska, L. Mazur, A. E. Koziol, J. Banachiewicz, M. Ucherek, M. Kandefer-Szerszen, *Monatsh. Chem.* **2009**, *140*, 439; j) S. Arfaie, A. Zarghi, *Eur. J. Med. Chem.* **2010**, *45*, 4013; k) L. Filippelli, C. O. Rossi, N. A. Uccella, *Colloids Surf. B* **2011**, *82*, 13; l) M. Nagaki, T. Ichijo, R. Kobashi, Y. Yagihashi, T. Musashi, J. Kawalami, N. Ohya, T. Goth, H. Sagami, *J. Mol. Catal. B* **2012**, *80*, 1.
- [2] J. Zhang, Z. Zhang, US-2010/0210675A1.
- [3] a) R. Vlegaar, *Pure Appl. Chem.* **1986**, *58*, 239; b) L. Leite, D. Jansone, M. Veveeris, H. Cirule, Y. Popelis, G. Melikyan, A. Avetisyan, E. Lukevics, *Eur. J. Med. Chem.* **1999**, *34*, 859; c) I. J. S. Fairlamb, L. R. Marrison, J. M. Dickinson, F.-J. Lu, J. P. Schmidt, *Bioorg. Med. Chem.* **2004**, *12*, 4285; d) A. Ripka, G. Shapiro, R. Chesworth, WO 2009/158393A1; e) A. Arcadi, S. Cacchi, F. Marinelli, P. Pace, *Synlett* **1993**, *10*, 743.
- [4] For reviews on the use of triple bonds in organocatalysis, see: a) A. Fraile, A. Parra, M. Tortosa, J. Alemán, *Tetrahedron* **2014**, *70*, 9145; b) R. Salvio, M. Moliterno, M. Bella, *Asian J. Org. Chem.* **2014**, *3*, 340.
- [5] For *Z* selectivity, see: a) Z. Wang, Z. Chen, S. Bai, W. Li, X. Liu, L. Lin, X. Feng, *Angew. Chem. Int. Ed.* **2012**, *51*, 2776; *Angew. Chem.* **2012**, *124*, 2830; b) Z. Zhang, X. Liu, Z. Wang, X. Zhao, L. Lin, X. Feng, *Tetrahedron Lett.* **2014**, *55*, 3797; c) Z. Wang, Z. Zhang, Q. Yao, X. Liu, Y. Cai, L. Lin, X. Feng, *Chem. Eur. J.* **2013**, *19*, 8591; d) T. Misaki, K. Kawano, T. Sugimura, *J. Am. Chem. Soc.* **2011**, *133*, 5695; e) Z. Chen, M. Furutachi, Y. Kato, S. Matsunaga, M. Shibasaki, *Angew. Chem. Int. Ed.* **2009**, *48*, 2218; *Angew. Chem.* **2009**, *121*, 2252.
- [6] For *E* selectivity, see: a) X. Wang, M. Kitamura, K. Maruoka, *J. Am. Chem. Soc.* **2007**, *129*, 1038; b) Q. Lan, X. Wang, K. Maruoka, *Tetrahedron Lett.* **2007**, *48*, 4675; c) D. Uraguchi, K. Yamada, T. Ooi, *Angew. Chem. Int. Ed.* **2015**, *54*, 9954; *Angew. Chem.* **2015**, *127*, 10092; d) Y. Hasegawa, I. D. Gridnev, T. Ikariya, *Angew. Chem. Int. Ed.* **2010**, *49*, 8157; e) G. Kang, Q. Wu, M. Liu, Q. Xu, Z. Chen, W. Chen, Y. Luo, W. Ye, J. Jiang, H. Wu, *Adv. Synth. Catal.* **2013**, *355*, 3131.
- [7] a) M. Bella, K. A. Jørgensen, *J. Am. Chem. Soc.* **2004**, *126*, 5672; b) H. E. Zimmermann, A. Pushechnikov, *Eur. J. Org. Chem.* **2006**, 3491; c) Q. Lan, X. Wang, S. Shirakawa, K. Maruoka, *Org. Process Res. Dev.* **2010**, *14*, 684; d) T. Misaki, N. Jin, K. Kawano, T. Sugimura, *Chem. Lett.* **2012**, *41*, 1675.
- [8] For selected papers on the aminocatalytic functionalization of alkynals, see: a) X. Zhang, S. Zhang, W. Wang, *Angew. Chem. Int. Ed.* **2010**, *49*, 1481; *Angew. Chem.* **2010**, *122*, 1523; b) J. Alemán, A. Núñez, L. Marzo, V. Marcos, C. Alvarado, J. L. García Ruano, *Chem. Eur. J.* **2010**, *16*, 9453; c) J. Alemán, C. Alvarado, V. Marcos, A. Núñez, J. L. García Ruano, *Synthesis* **2011**, *12*, 1840; d) J. Alemán, A. Fraile, L. Marzo, J. L. García Ruano, C. Izquierdo, S. Díaz-Tendero, *Adv. Synth. Catal.* **2012**, *354*, 359; e) X. Cai, C. Wang, J. Sun, *Adv. Synth. Catal.* **2012**, *354*, 359; f) X. Zhang, X. Song, H. Li, S. Zhang, X. Chen, X. Yu, W. Wang, *Angew. Chem. Int. Ed.* **2012**, *51*, 7282; *Angew. Chem.* **2012**, *124*, 7394.
- [9] For aminocatalytic systems, see: a) K. S. Halskov, B. S. Donslund, B. Matos-Paz, K. A. Jørgensen, *Acc. Chem. Res.* **2016**, *49*, 974; for noncovalent interactions in organocatalysis, see: b) S. E. Wheeler, T. J. Seguin, Y. Guan, A. C. Doney, *Acc. Chem. Res.* **2016**, *49*, 1061; c) D. M. Walden, O. M. Ogba, R. C. Johnston, P. H.-Y. Cheong, *Acc. Chem. Res.* **2016**, *49*, 1279.
- [10] H. E. Zimmerman, *J. Org. Chem.* **1955**, *20*, 549.
- [11] We have analyzed the enantioselectivity obtained in the created chiral centers with both types of catalysts (steric and hydrogen-bond types). However, the diastereoisomer (*E* or *Z*) obtained as the major one in each case exhibited a low enantiomeric excess (<20%), whereas it was much better (*ee* > 60%) for the geometric isomers obtained as the minor in the mixture. Additionally, the catalysts affording better *Z/E* stereocontrol were not the same as those providing better *ee*. Therefore, we have not paid attention to the enantioselectivity in the rest of the work.
- [12] The decrease of the catalyst loading to 10 or 5 mol% resulted in a decrease in the reactivity and the diastereoselectivity.
- [13] Reaction of **2E** under conditions of Table 2 gave a 28:72 mixture of *Z/E* isomers. This is the only case in which these conditions did not produce the *Z* isomer as the major component of the reaction mixture.
- [14] It is known that Meldrum 's derivatives bearing a formyl group at the appropriated position can undergo rearrangements resulting in a six-membered ring, see ref. [3e].
- [15] See, for example, a) H. Newman, R. B. Angier, *J. Org. Chem.* **1966**, *31*, 1456; b) H. Newman, A. Howard, R. B. Angier, *J. Org. Chem.* **1966**, *31*, 1462; c) K. C. Nicolaou, T. Montagnon, G. Vassilikogiannakis, C. J. N. Mathison, *J. Am. Chem. Soc.* **2005**, *127*, 8872; d) H.-S. Yeom, Y. Lee, J. Jeong, E. So, S. Hwang, J.-E. Lee, S. S. Lee, S. Shin, *Angew. Chem. Int. Ed.* **2010**, *49*, 1611; *Angew. Chem.* **2010**, *122*, 1655; e) E. Li, Y. Huang, L. Liang, P. Xie, *Org. Lett.* **2013**, *15*, 3138.
- [16] The structure of **8** was determined by X-ray crystal analysis: CCDC 1043200 (**8**) contains the supplementary crystallographic data for this paper. These data are provided free of charge by The Cambridge Crystallographic Data Centre.
- [17] Firstly, we observed that the δ values of the aldehydic proton of the compounds obtained as the major product under the conditions in Tables 2 and 3, are lower than those resulting from the conditions in Tables 5 and 6. In the case of the olefinic protons, δ values of compounds in Tables 2 and 3 are higher than those of Tables 5 and 6. This allowed us to confirm that the compounds in Tables 2 and 3 have the same configuration and were different to the compounds in Tables 5 and 6.

Received: July 20, 2016
Published online on ■■■■■, 0000

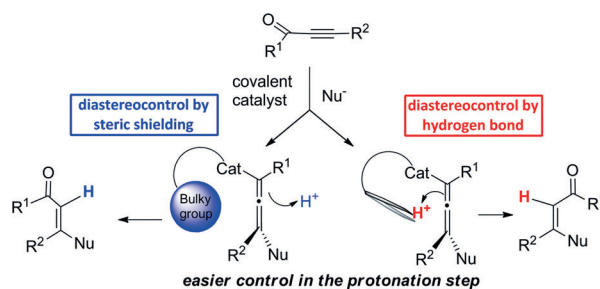
FULL PAPER

Organic Synthesis

L. Marzo, J. Luis-Barrera, R. Mas-Ballesté,
J. L. G. Ruano, J. Alemán*

■■■ - ■■■

Stereodivergent Aminocatalytic Synthesis of Z- and E-Trisubstituted Double Bonds from Alkynals



Diastereoselectivity: A highly diastereo-
selective synthesis of trisubstituted Z- or
E-enals, which are important intermedi-
ates in organic synthesis, as well as
being present in natural products, is de-

scribed using different alkynals and nu-
cleophiles as starting materials (see
scheme). Diastereocontrol is mainly gov-
erned by the appropriate catalyst (hy-
drogen bonding versus steric effects).